The Abdus Salam
International Centre for Theoretical Physics

United Nations
Educational, Scientific
and Cultural Organization

International Atomic
Energy Agency

SMR 1673/39

AUTUMN COLLEGE ON PLASMA PHYSICS

5 - 30 September 2005

Ion Acceleration in Laser Produced Plasmas: High Efficency Regimes and Applications

F. PEGORARO

Universita' di Pisa, Italy

Ion acceleration in laser produced plasmas: high efficency regimes and applications

Francesco Pegoraro

Abstract

The high efficiency ion acceleration obtained in experiments with petawatt laser pulses interacting with solid targets opens the way to applications, such as laser produced fast ion beam injection into conventional accelerators and hadron therapy in oncology, together with the possibility of developing high-energy-physics (HEP) facilities in conjunction with projects for inertial confined nuclear fusion (ICF) and neutron spallation sources.

Physics Department University of Pisa pegoraro@df.unipi.it

Introduction

The effective ion acceleration during the interaction of an ultra short and ultra intense laser pulse with matter is possibly one of most important results in the investigation of the interaction of multi-terawatt and petawatt power laser pulses with plasmas.

G. Mourou, et al., Physics Today **51**, *22 (1998);*

G. Mourou,et al., Plasma Phys. Rep. **28**, *12 (2002).*

Collimated beams of fast protons have been produced in recent experiments where electron energies in the hundreds of MeV range were observed while the protons have a broad spectrum, with maximum energies up to a few tens of MeV.

A. Maksimchuck et al., Phys. Rev. Lett. **84** *(2000) 4108;*

E. L. Clark et al., Phys. Rev. Lett. **85** *(2000) 1654;*

S. P. Hatchett et al. Phys. Plasmas **7** *(2000) 2076;*
R. A. Snavely et al., Phys. Rev. Lett. **85** *(2000) 2945;*
A. J. Mackinnon et al., Phys. Rev. Lett. **86** *(2001) 1769;*
M. Hegelich et al., Phys. Rev. Lett. **89** *(2002) 085002.*
M. Roth,et al., Phys. Rev. Special Topics, **AB 5**, *061301 (2002)*
M. Zepf, et al., Phys. Rev. Lett. 90, 064801 (2003).

Compared to conventional accelerators these proton beams have a very high brilliance and are very directional, with a divergence of a few degrees at the highest energies and an apparent source size of less than $5 - 10\ \mu m$.

The number of particles in the beams can approach 10^{13} with good conversion efficiency of the laser energy into the energy of fast ions. The beams are emitted in bursts of ps duration, three orders of magnitude shorter than conventional accelerator bunches.

These laser-produced ion beams have important applications ranging from the fast ignition of thermonuclear targets, to proton imaging, deep proton lithography, medical physics, and injectors for conventional accelerators.

Although the basic physical mechanisms of ion beam generation in the plasma produced by the laser pulse interaction with the target are common to all these applications, each application requires a specific optimization of the ion beam properties i.e., an appropriate choice of the target design and of the laser pulse intensity, shape and duration.

As recently stressed, different ion acceleration regimes are encountered in the interaction of ultraintense laser pulses with a target.

S.V. Bulanov, et al., Plasma Phys. Reports 30, 196 (2004).

Acceleration regimes and beam properties

When laser pulses with powers corresponding to relativistically strong fields are used we find a transition from an essentially quasineutral, lower intensity regime where the heated Boltzmann electrons accelerate the ions up to energies, per ion unit charge, of the order of the electron temperature[1] to a new regime where dynamical charge separation effects are dominant and a fraction of the ions can acquire an energy that is substantially larger than the electron thermal energy.

Extensive investigations with multi-dimensional Particle In Cell simulations have confirmed that collimated beams of fast protons with energies in the several MeV range can be obtained by optimizing the laser-target parameters.

[1] see e.g. P. Mora, Phys. Rev. Lett. **90**, 185002 (2003).; S. Betti, F. Ceccherini, F. Cornolti, F. Pegoraro, *Plasma Phys. Contr. Fus.*, **47**, 521 (2005); F. Cornolti, F. Ceccherini, S. Betti, F. Pegoraro, *Phys. Rev. E* 71, 056407-1 (2005).

T. Esirkepov, et al., JETP Lett. **70**, *82 (1999);*
S. Bulanov, et al., JETP Lett. **71**, *407 (2000);*
Y. Sentoku,et al., Phys. Rev, **E 62**,*7271 (2000);*
H. Ruhl, et al., Plasma Phys. Rep. **27**, *411 (2001);*
Y. Sentoku,et al., Appl. Phys. **B 74**, *207 (2002);*
T. Nakamura, Phys. Rev, **E 67**, *026403, (2003).*
T. Esirkepov,et al., Phys. Rev. Lett. **89**, *175003 (2002);*
S. Bulanov,et al., Plasma Physics Reports, **28**, *975 (2002).*

As an example, here we recall the numerical results of the 3-D simulations of the interaction of an ultrashort ultra intense laser pulse with a plasma slab reported in *F. Pegoraro, et al., IEEE Trans. Plasma Science,***28**, *1226, (2000).* .

The aim of these simulations was to find the maximum energy that the ions can gain in the fields created by the nonadiabatic interaction on the laser pulse with the plasma.

Two acceleration phases were identified: a first phase when the ions propagate inside the partly evacuated channel along the pulse path and are accelerated by a relativistically propagating double layer structure, and a second phase where they are accelerated in vacuum after they exit the slab both electrostatically due to the expansion of the plasma electron cloud and electromagnetically du to the expansion of the self-generated magnetic field carried by the plasma.

A short (15λ) plasma slab with $\omega/\omega_p = 1$ was considered with ω_p is the nonrelativistic unperturbed plasma frequency and mass ratio corresponding to a hydrogen plasma. The pulse was circularly polarized with amplitude $a_{\rm e} \simeq 50$, slightly larger than the square root of the mass ratio, the pulse length is 20λ and its width is 10λ. In these 3-D run 8 particles per species, per cell were used (the total number per species was ~ 18.5 millions).
The formation of the channel in the ion density in the 3-D plasma slab is shown in Fig.1 at $t = 30$ projected on the horizontal x-y plane at $z = 0$, frame (a), and on the transverse y-z plane at $x = 15\lambda$, frame (b).

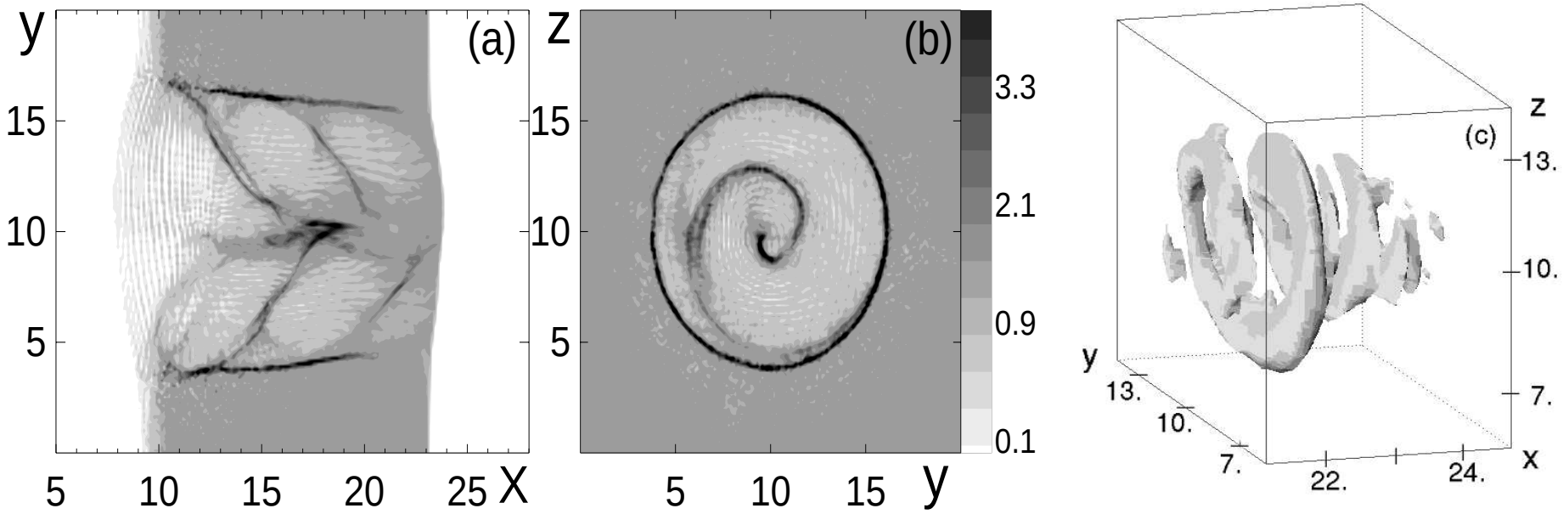

Figure 1: The x-y distribution at $z = 0$ (a), the y-z distribution (b) of the ion density at $x = 15\lambda$ and the isosurface $\sqrt{(E^2 + B^2)/2} = 40$ of the electromagnetic energy density (c) in the case of the pulse propagating in the 3-D plasma slab.

The circularly polarized pulse has carved a staircase structure which resembles the helical chamber inside a shell.
A similar helix, although less sharp, is also seen in the electron density and in Fig.1c where the isosurface of the electromagnetic energy density corresponding to the amplitude value $\sqrt{(E^2 + B^2)/2} = 40$ is shown.

The expansion and acceleration of the ions in the vacuum region, following the electron expansion when the pulse has drilled a hole through the slab, is shown in Fig.2 at $t = 48$.
The $x - y$ section at $z = 0$ of the ion density distribution shows a strongly collimated beam along the x axis.
This beam collimation is also seen in the 3-D plot where the isosurface corresponding to $n_i = 1.8$ is shown.
We see that the beam is strongly collimated.
The longitudinal ion momentum distribution at $t = 48$ is shown in Fig.2c.

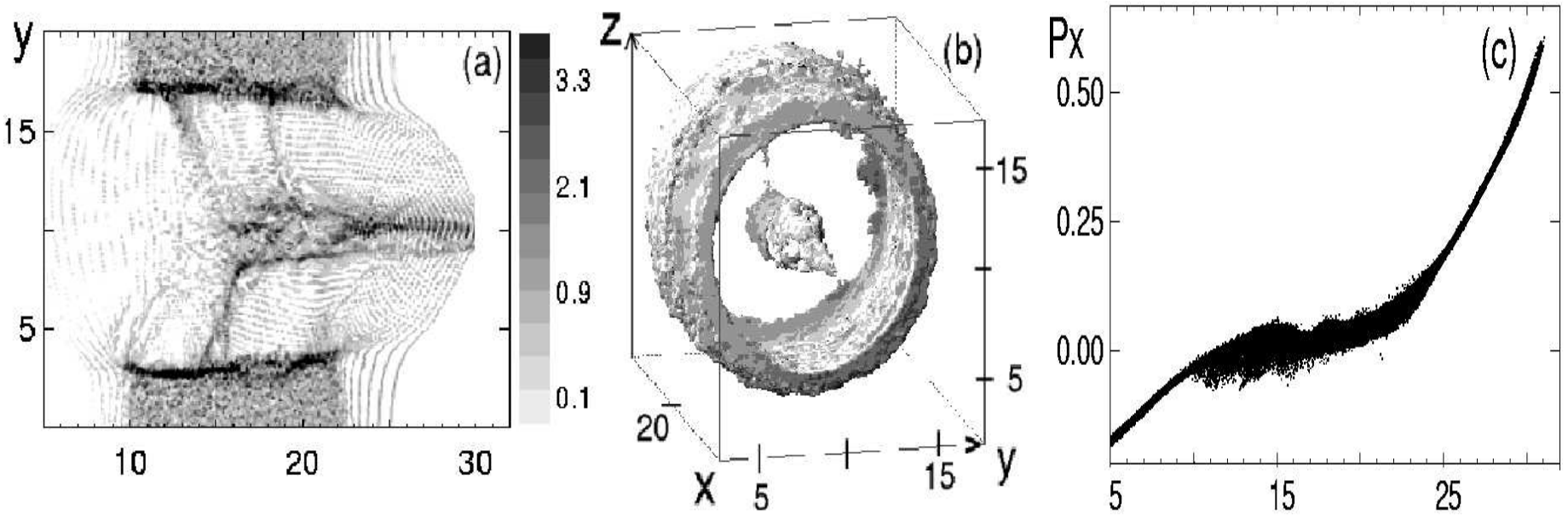

Figure 2: The x-y distribution at $z = 0$ (a), and the isosurface $n_i = 1.8$ of the ion density (b) at $t = 48\ (2\pi/\omega)$, the ion phase space (P_x, x) (frame c) in the case of the pulse propagating in the 3-D plasma slab.

Besides the maximum energy reached, an important issue in the investigation of the different ion acceleration mechanisms, is the quality of the beam produced in terms of spatial collimation and in particular of energy resolution.

The proton beams that are obtained in current experiments do indeed provide a novel and effective diagnostic tool for detecting the electromagnetic fields generated by the laser pulse in the plasma[2] but, because of their broad 'thermal' energy spectra, such beams are not appropriate for applications where energy selection is an issue.
This is of particular importance when the use of laser accelerated proton beams is proposed in order to provide a controlled and localized delivery of energy, such as in the scheme of the proton driven fast ignition [3] of a thermonuclear pellet or

[2] see M. Borghesi, *et al.*, Plasma Phys. Control. Fus. **43**, A267 (2001); M. Borghesi *et al.*, Phys. Rev. Lett., **88**, 135002 (2002).

[3] M. Roth, *et al.*, Phys. Rev. Lett. **86**, 436 (2001); S. Atzeni, et al., Nucl. Fusion **42**, L1 (2002); M. Temporal, *et al.*, Phys. Plasmas **9**, 3098 (2002).

in the applications to hadrontherapy in oncology [4].

Proton imaging employs proton beams as a diagnostic tool in a point-projection imaging scheme (see Fig.6a) and provides the possibility of identifying electric fields in dense plasmas and laser-irradiated targets with unprecedented spatial and temporal resolution.

M. Borghesi, et al., Plasma Phys. Control. Fus. **43**, *A267 (2001)*

The proton beams need not be monochromatic for this application, indeed a broad spectrum can be advantageous, as it allows multiframe capability.
The targets used for proton beam production are thin foils that act as the source of the proton beam. The electro-magnetic fields in a plasma between the source and the detector distort the geometrical propagation of the protons.

[4].Khoroshkov,*et al.*, Eur. J. Phys **19**, 523 (1998); G. Kraft, Physica Medica XVII, Suppl. **1**, 13 (2001); U. Amaldi, Physica Medica XVII, Suppl. **1**, 33 (2001); M. Goiten, *et al.*, Phys. Today **55**, 45 (2002).S. Bulanov *et al.*, Plasma Phys. Rep. **28**, 453 (2002); S. Bulanov*et al.*, Phys. Lett. **A 299**, 240 (2002).

In this way electric fields, slowly varying on the proton crossing time, can be detected with micron spatial resolution and their evolution can be followed on a picosecond time scale.

This high temporal resolution makes laser produced proton beams ideal in order to detect coherent field structures arising from the nonlinear plasma dynamics following intense, short pulse interactions.

The potentialities of this method are apparent from the results shown in Fig.3 on the time evolution of the sheath electric field at the rear side of the target[5].

[5] M. Borghesi, 2005, in press

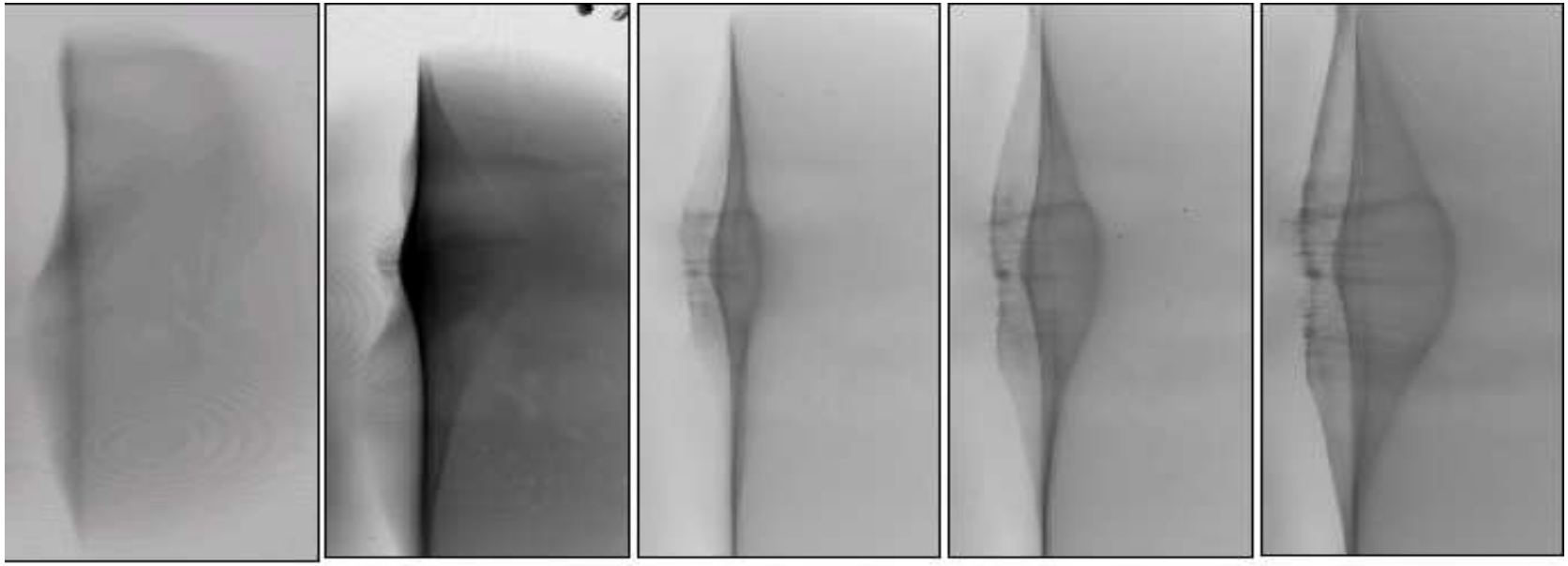

Field due to plasma sheath at the rear surface
Borghesi et al in press

Figure 3:

Oncological proton therapy and double layer targets

The use of protons in radiotherapy for cancer treatment has several advantages:
i) the proton beam scattering on the atomic electrons is weak and thus there is less irradiation of healthy tissues in the vicinity of the tumor,
ii) the slowing down length for a proton with given energy is fixed, which avoids undesirable irradiation of healthy tissues at the rear side of the tumor,
iii) the well localized maximum of the proton energy losses in matter (the Bragg peak) leads to a substantial increase of the irradiation dose in the vicinity of the proton stopping point.

However the construction and operation costs of hospital-based proton therapy centers remain comparatively higher than those of the most expensive conventional beam therapy plants designed for radiation therapy.

An attractive possibility of reducing such costs is to use ultrashort, ultraintense laser pulses to produce the proton beams. In this scheme the laser radiation is delivered to the target where its energy is converted into the energy of fast protons. In this approach the central accelerator, the channels through which the fast protons are transported and most of the gantry, which provides multi-directional irradiation of a laying patient, is no longer required.
The basic parameters required for a proton beam to be used for medical applications can easily be reached with present accelerator technology. The proton beam intensity must be in the 10^{10} to 5×10^{10} protons per second range, the maximum proton energy must be in the 230 to $250 MeV$ range. For laser accelerators the most demanding conditions are the requirement for a highly monoenergetic proton beam with $\Delta\mathcal{E}/\mathcal{E} = 10^{-2}$ and the system duty factor i.e., the fraction of the time during which the proton beam can be used which is important in determining the economical feasibility of the use of a laser accelerator.

The main physical challenge is to devise a method of producing proton beams of sufficiently high quality in terms of energy resolution to ensure that a substantially high and homogeneous dose is delivered to the tumor while sparing neighboring healthy tissues.

A possible method of achieving such high quality proton beams. The basic idea behind this proposal is to make the interaction between the laser pulse and the plasma strongly non adiabatic by using short laser pulses and a target made of a layer of heavy ions followed by a thin proton layer with a transverse size smaller than the pulse waist.

S. Bulanov et al., Plasma Phys. Rep. **28**, *453 (2002);*
S. Bulanov et al., Phys. Lett. **A 299**, *240 (2002).*

Double layer targets were shown experimentally[6] to provide a considerable increase in energies and current of protons produced.

[6] J. Badziak, *et al.*, Phys. Rev. Lett., **87**, 215001 (2001); J. Badziak,*et al.*, J. Appl. Phys., **91**, 5504 (2002).

In this layered target scheme a foil is used as the target and its rear surface is coated with a thin and transversally narrow hydrogen layer, Fig.4.

An ultrashort ultraintense laser pulse irradiates the target: the heavy atoms are partly ionized and most of the resulting free electrons abandon the foil. This leads to a large electric field due to charge separation.
Heavy ions with large mass to charge ratio remain at rest while the protons in the coating are accelerated. If the proton coating is thin and has a transverse size smaller that the diameter of the focal spot of the laser pulse, this scheme provides a controlled acceleration of protons.

The electrons escaping the heavy ion foil under the action of the ponderomotive pressure of the laser radiation give rise to a quasistatic electric field caused by the non-neutralized electric charge. This field is localized in a finite region with dimensions comparable to the transverse dimension of the laser pulse. I

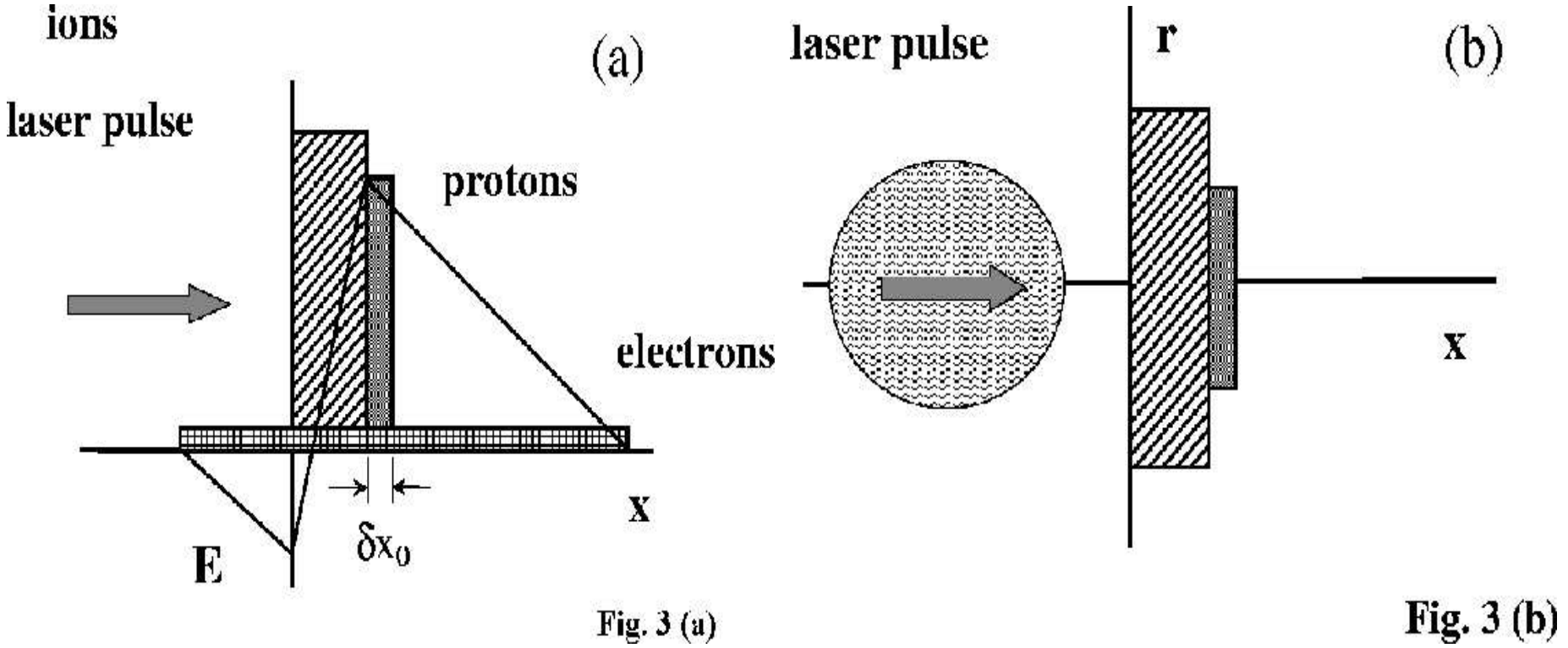

Figure 4: Two-layer target. The rear side of the foil of heavy ions is coated with a thin hydrogen layer.

In this initial stage the protons are accelerated by this electric field before the heavy ions of the first layer start to move.
If the total number of protons is small in comparison with the number of electrons that have escaped from the target, the effect of the electric field of the protons on their dynamics can be neglected.
In this case the proton acceleration can be described in the approximation of test particles moving in an assigned electric field.
The energy of these protons can approach $2m_pc^2a_0^2$ where $a_0 = eE_0/m_ec\omega_0$ is the dimensionless amplitude of the laser pulse, m_p is the proton mass and the energy of the electrons in the cloud has been estimated to be of the order of $a_0m_ec^2$, as consistent with the non adiabatic nature of the interaction between the laser pulse and the electrons laser.

For $a_0 \simeq 1$, which corresponds for a $\lambda \approx 1\mu m$ pulse wavelength to a laser intensity of the order of $10^{18}\ Watt/cm^2$, the electrons can reach energies up to several Mev, while the energy of the fast ions can be as high as $\sim 1\ Gev$.

Although the 1-D approximation overestimate the energies achievable, these results indicate that with a proper optimization of the interaction conditions, one can achieve high proton energies even with modest laser pulse intensities.

These analytical considerations are supported by detailed numerical simulation reported in

S. Bulanov et al., Plasma Phys. Rep. **28**, *453 (2002);*

S. Bulanov et al., Phys. Lett. **A 299**, *240 (2002);*

S.V. Bulanov, et al., submitted to Plasma Phys. Reports (2003).

A regime of ion acceleration that exhibits very favourable properties has been recently identified along these lines in

T. Zh. Esirkepov, et al., Phys. Rev. Lett. **92** *(2004) 175003.*

S. V. Bulanov, et al., Plasma Phys. Rep. ***30*** *(2004) 196.*

In this regime the radiation pressure of the electromagnetic wave plays a dominant role in the interaction of an ultraintense laser pulse with a foil.

In this Radiation Pressure Dominant (RPD) regime the ion acceleration appears to be due to the radiation pressure of the laser light on the electron component with the momentum being transferred to the ions through the electric field arising from charge separation.

In the RPD regime the proton component moves forward with almost the same velocity as the average longitudinal velocity of the electron component.

Thus the proton kinetic energy is well above that of the electron component.

In addition in the RPD regime the ion acceleration mechanism is found to be highly efficient, and, as we will show explicitly, the ion energy per nucleon is proportional to the laser pulse energy.

Radiation Pressure-dominated (RPD) regime: 1D analytical description

The RPD acceleration mechanism can be explained as follows.
When this regime is reached, the accelerated foil, which consists of the electron and proton layers, can be regarded as a relativistic plasma mirror co-propagating with the laser pulse.
Let us assume that the laser pulse is perfectly reflected from this mirror.
As a result of the reflection at the co-propagating relativistic mirror, the frequency of the electromagnetic wave decreases by the factor of

$$(1 - v/c) \,/\, (1 + v/c) \approx 1/4\gamma^2,$$

where v is the mirror velocity and $\gamma = \left(1 - v^2/c^2\right)^{-1/2}$.

The length of the reflected pulse is longer by $4\gamma^2$.

Its electric field is smaller by $4\gamma^2$.

Hence, when this regime is reached, the plasma mirror acquires the energy

$$(1 - 1/4\gamma^2)\mathcal{E}_{las,in}$$

from the laser, where $\mathcal{E}_{las,in}$ is the energy in the incident pulse.
In this stage the radiation pressure of the light accelerates the plasma slab (electrons and protons).

The radiation momentum is transferred to the protons through the charge separation field and the kinetic energy of the protons is much greater than that of the electrons.

Note that the pulse frequency in the foil frame decreases as the velocity of the foil

plasma foil approaches the speed of light; this makes the mirror effect increasingly more effective.

In addition foil instabilities, as seen in the laboratory frame, are slowed down because of the relativistic dilation of time.

It is possible to show how this regime is achieved and to estimate the proton maximum energy and the acceleration efficiency using the model of the flat foil driven by the e.m. radiation pressure.

The radiation pressure is given by:

$$P = \frac{E_0'^2}{2\pi} = \left(\frac{\omega'}{\omega}\right)^2 \frac{E_0^2}{2\pi} = \frac{E_0^2}{2\pi}\left(\frac{c-v}{c+v}\right). \qquad (1)$$

Here $v = dx/dt$ is the foil instantaneous velocity, i.e.

$$\frac{dx}{dt} = c\frac{p}{(m_p^2c^2 + p^2)^{1/2}}. \tag{2}$$

Primed (unprimed) quantities refer to the moving (laboratory) reference frame. In a quasi-one-dimensional geometry, the laser electric field at the foil location $x(t)$ depends on time as $E_0' = E_0(t - x(t)/c)$.
Since the expression of the radiation pressure is the same in both frames, we can write the equation of motion of the foil as

$$\frac{dp}{dt} = \frac{E_0^2(t - x(t)/c)}{2\pi n_0 l_0}\frac{(m_p^2c^2 + p^2)^{1/2} - p}{(m_p^2c^2 + p^2)^{1/2} + p}, \tag{3}$$

where p is the momentum of the proton representing the foil, l_0 and n_0 are the thickness and initial proton density of the foil.

In the simplest case, when the laser pulse is assumed to be long enough and with a homogeneous amplitude, we can consider the electric field in Eq. (3) to be constant: $E_0 = \mathrm{const}$.
Its solution $p(t)$ is an algebraic function of time t. For the initial condition $p = 0$ at $t = 0$ it can be written in the implicit form

$$\frac{2p^3 + 2(m_p^2c^2 + p^2)^{3/2}}{3m_p^2c^2} + p - \frac{2}{3}m_pc = \frac{E_0^2}{2\pi n_0 l_0}t. \tag{4}$$

At the initial stage, for $t \ll 2\pi n_0 l_0 m_p c/E_0^2$, the proton momentum is a linear function of time: $p \approx (E_0^2/2\pi n_0 l_0)t$.
As $t \to \infty$, the dependence of the accelerated proton momentum on time changes asymptotically to

$$p \approx \mathcal{E}_{p\mathrm{kin}}/c \approx m_pc\ (3E_0^2t/8\pi n_0 l_0 m_p c)^{1/3}. \tag{5}$$

To find an upper limit to the proton energy acquired during the interaction with a laser pulse of finite duration, we must include the dependence of the laser electromagnetic field on time t and on the coordinate x. Because of the foil motion, the interaction time can be much longer that the laser pulse duration. We introduce the phase of the wave $\psi = \omega_0(t - x(t)/c)$, as a new variable, ω_0 being the incoming laser frequency. Using Eq.(2), we cast Eq.(3) for the particle momentum in the form

$$\frac{dp}{d\psi} = \frac{E_0^2(\psi)}{2\pi\omega_0 n_0 l_0} \frac{(m_p^2c^2 + p^2)^{1/2}}{(m_p^2c^2 + p^2)^{1/2} + p} \tag{6}$$

Its solution reads

$$p = m_p c \frac{w(w+1)}{(w+1/2)}\,, \quad \text{where} \quad w(\psi) = \int_{-\infty}^{\psi} \frac{E_0^2(s)}{4\pi\omega_0 n_0 l_0 m_p c} ds\,. \tag{7}$$

Using the definition of ψ and (7) we can find the dependence of the foil coordinate on time and write the equations for t and x as functions of the variable ψ in the form

$$\frac{dt}{d\psi} = \frac{1}{\omega_0}\left(\frac{c}{c-v}\right) = \frac{1}{\omega_0}\frac{(m_p^2c^2+p^2)^{1/2}}{(m_p^2c^2+p^2)^{1/2}-p} = \frac{1}{\omega_0}\left[1+2w(w+1)\right] \qquad (8)$$

and

$$\frac{dx}{d\psi} = \frac{dx}{dt}\frac{dt}{d\psi} = \frac{c}{\omega_0}2w(w+1). \qquad (9)$$

The function $w(\psi)$ can be interpreted as the normalized energy of the portion of the laser pulse that has interacted with the moving foil by time t.
The maximum value of $w(\psi)$ is $w_{\max} = \mathcal{E}_{las,in}/\mathcal{N}_p m_p c^2$, where $\mathcal{E}_{las,in}$ is the laser pulse energy, $\mathcal{N}_p = n_0 l_0 S$ is the number of protons in the region of the foil irradiated by the laser pulse.

From the solution of Eq. (3) given by Eq. (7) in terms of w we obtain for the kinetic energy of a proton initially at rest

$$\mathcal{E}_{p\mathrm{kin}} \equiv (m_p^2 c^2 + p^2)^{1/2} c - m_p c^2 = m_p c^2 w^2/(w + 1/2). \tag{10}$$

In the limits $w \ll 1$ and $w \gg 1$, we have respectively $\mathcal{E}_{p\mathrm{kin}} \approx 2 m_p c^2 w^2$, and $\mathcal{E}_{p\mathrm{kin}} \approx m_p c^2 w$.

The upper limit to the proton kinetic energy and, correspondingly, to the efficiency of the laser-to-proton energy transformation can be obtained from Eq. (10) by setting $w = w_{\mathrm{max}}$:

$$\mathcal{E}_{p\mathrm{kin,max}} = \frac{2\mathcal{E}_{las,in}}{2\mathcal{E}_{las,in} + \mathcal{N}_p m_p c^2} \frac{\mathcal{E}_{las,in}}{\mathcal{N}_p} \,. \tag{11}$$

We see that within this model almost all the energy of the laser pulse is transformed into the energy of the protons if $\mathcal{E}_{las,in} \gg N_p m_p c^2/2$.

The acceleration length $x_{acc} \approx ct_{acc}$ and the acceleration time t_{acc} can be estimated using Eq.(11) and the $t^{1/3}$ asymptotic dependence of the proton energy on time as

$$t_{acc} \approx \frac{2}{3}\left(\frac{\mathcal{E}_{las,in}}{\mathcal{N}_p m_p c^2}\right)^2 \tau_{las,in}. \tag{12}$$

Within this simplified 1D approximation, the protons formally have a mono-energetic spectrum.

Processes such as the transverse inhomogeneity of the amplitude of the laser pulse, the electron stochastization due to "vacuum heating" and the subsequent proton layer expansion under the action of the Coulomb repelling force may result in the broadening of the proton energy spectrum or reduce the acceleration efficiency.

Numerical results

The study of three-dimensional effects requires the use of numerical simulations.[7]

The laser pulse is linearly polarized along the z-axis and propagates in the direction of the x-axis. Its dimensionless amplitude is $a = 316$, corresponding to the peak intensity $I = 1.37 \times 10^{23}\,\mathrm{W/cm^2} \times (1\,\mu\mathrm{m}/\lambda)^2$, $\lambda = 1\mu\mathrm{m}$ being the laser wavelength. The laser pulse is Gaussian with FWHM size $8\lambda \times 25\lambda \times 25\lambda$, so its energy is $\mathcal{E}_L = 10\,\mathrm{kJ} \times (1\,\mu\mathrm{m}/\lambda)^2$.
Protons are generated from a $1\mu m$ foil.
Due to the finite contrast of the laser, pulse pedestals reaching the target before the main pulse will pre-form a fully ionized plasma.

[7] The simulations under consideration have been performed with the code $REMP$ (Relativistic Electro-Magnetic Particle-mesh code) on 720 processors of the supercomputer HP Alpha server SC ES40 at JAERI Kansai and form the basis of the studies presented in *T. Zh. Esirkepov, et al., Phys. Rev. Lett.* **92** *(2004) 175003*

Thus the target behaves as a fully ionized, 1λ thick plasma with density $n_e = 5.5 \times 10^{22}\,\mathrm{cm}^{-3} \times (1\,\mu\mathrm{m}/\lambda)^2$, which corresponds to the Langmuir frequency $\omega_{pe} = 7\omega$.
The protons and the electrons have the same absolute charge and their mass ratio is $m_p/m_e = 1836$.
The simulation box size is $100\lambda \times 72\lambda \times 72\lambda$ corresponding to the grid size $2500 \times 1800 \times 1800$, so the mesh size is 0.04λ.
The total number of quasi-particles is 4.37×10^9.
The boundary conditions are periodic along the y- and z-axis and absorbing along the x-axis for both the e.m. radiation and the quasi-particles.

In the figures space and time units are the wavelength λ and period $2\pi/\omega$ of the incident radiation.

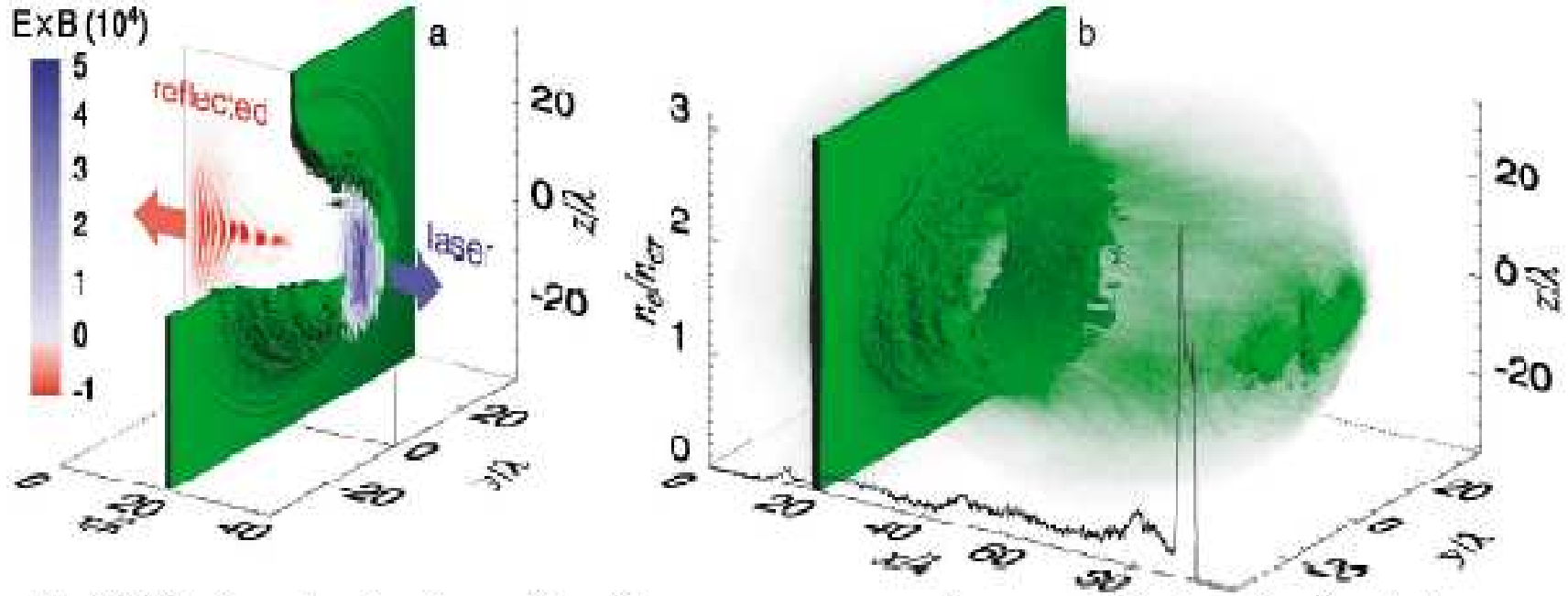

Figure. 5. (a) The ion density isosurface (a quarter removed to reveal its interior) and the x component of the normalized Poynting vector in the (x; y=0; z) plane. (b) The isosurface for $n = 2n_{cr}$, at $t = 100$; the black curve shows the ion density along the laser pulse axis.

Figure 5:

A region of the foil with the size of the laser focal spot is pushed forward.

Although the plasma in the foil is overcritical, it is initially transparent for the laser pulse due to the effect of relativistic transparency.

Therefore a portion of the laser pulse passes through the foil.

Eventually the pulse accelerates the electrons and, as a result of the charge separation, a longitudinal electric field is formed.

The dimensionless amplitude of the longitudinal field is $a_{\|} \approx 150$ corresponding to $E_{||} = 4.8 \times 10^{14}\,\mathrm{V/m} \times (1\,\mu\mathrm{m}/\lambda)$.
The typical distance over which charge separation occurs is comparable with the initial thickness of the foil and is much smaller than the transverse size of the region that is being pushed.

The proton layer is accelerated by this longitudinal field.

The laser pulse frequency in the reference frame comoving with the accelerated plasma region decreases as time progresses so that the accelerating foil become less transparent with time.

The thickness of coloured stripes, which corresponds to half of the radiation wave length, increases from left to right in the reflected part of the pulse (along the x-axis). This increase is weaker at the periphery (in the transverse direction). This 'nonuniform red shift' results from the Doppler effect when the laser light is reflected from the co-propagating relativistic mirror which accelerates and deforms in time.

The red shift shows that the laser pulse does indeed lose its energy by accelerating the plasma mirror.

The accelerated protons form a nearly flat "plate" at the front of the electron "cocoon".

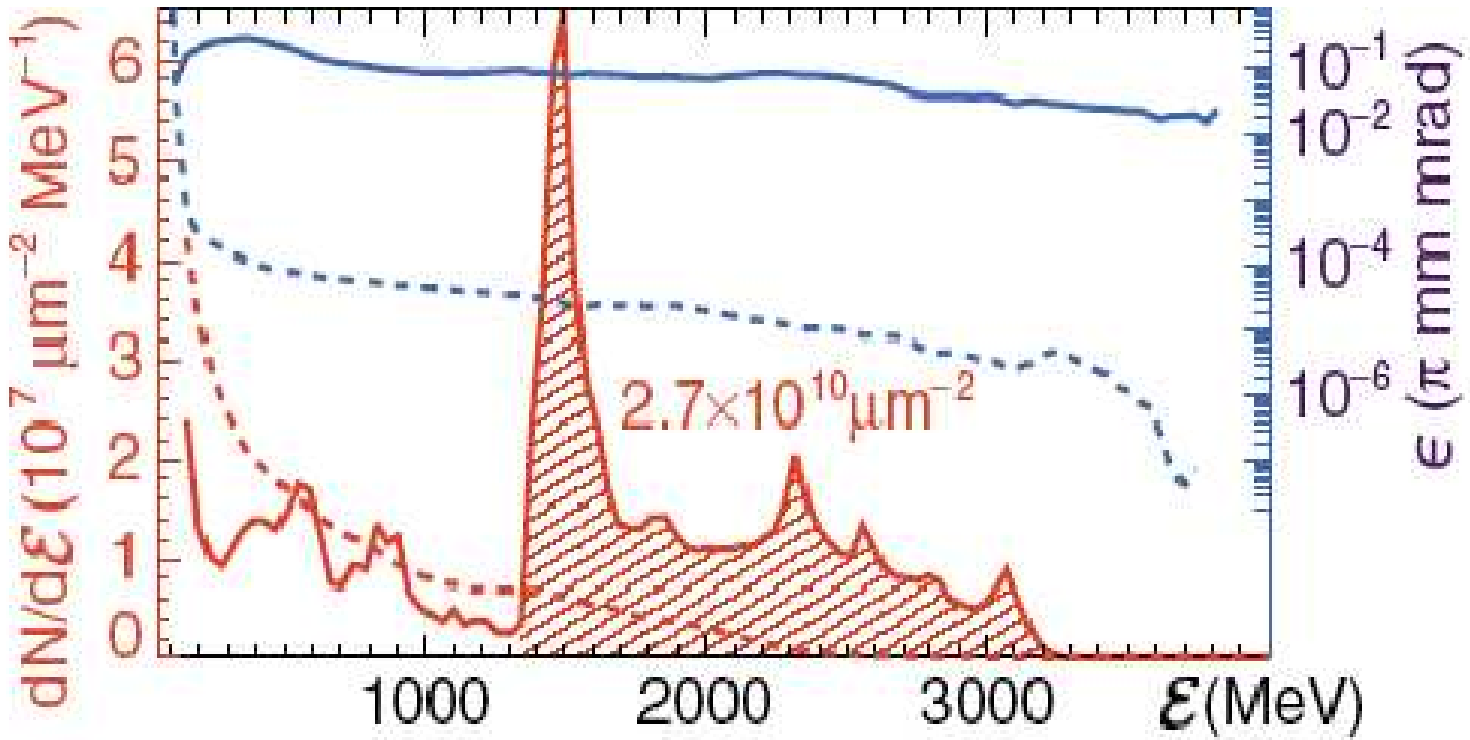

Figure 6. The energy spectrum (red) and transverse emittance (blue) of ions (solid) and electrons (dashed)

Figure 6:

Fig.6 shows the maximum proton energy versus time. This dependence is initially linear and, at later times, the maximum proton energy scales as $t^{1/3}$ as predicted by the 1D analytical model.
The protons in the plate structure are accelerated according to the RPD regime. Considering all accelerated protons the laser-to-proton energy transfer efficiency is of the order of 40% and it reduces to 12% if only protons with $E > 1\ GeV$ are included. About 2.7×10^{10} proton/μm^2 are accelerated.

These simulations provide numerical evidence of the fact that the RPD acceleration mechanism should appear already for laser intensities of 10^{23}W/cm^2. The time evolution is hydrodinamically stable and the acceleration highly efficient.

The radiation-pressure dominated acceleration regime may offer a stable and efficient operation regime for laser-driven proton boosters. This acceleration regime provides the opportunity to develop these facilities in conjunction with projects for inertial confinement fusion (ICF) and neutron spallation sources.

Conclusions

As a concluding remark I wish to stress the fundamental role that the numerical simulations play in the analysis of these "extreme" regimes which are outside the reach of most analytical developments because of their high dimensionality and because of their full nonlinear dynamics.
Simulations here are not only used for validating analytical models, but also play the more vital role of an investigative tool for discovering new phenomena.
Obviously this simulation analysis must be accompanied by the development of an appropriate terminology, in order to describe the numerical results, and must be guided by an "a priori" understanding of the relevant range of parameters and their scaling. Both the terminology and the parameter estimates can only be obtained from a physical understanding based on the extrapolation of simplified, lower dimensionality, models.